A novel method for determining the small-strain shear modulus of soil using the bender elements technique

Yejiao Wang, Nadia Benahmed, Yu-Jun Cui, Anh Minh A.M. Tang

A novel method for determining the small-strain shear modulus of soil using bender elements technique

Yejiao WANG[1], Nadia BENAHMED[2], Yu-Jun CUI[1], Anh Minh TANG[1]

1: Ecole des Ponts ParisTech, U.R. Navier/CERMES, 6 – 8 av. Blaise Pascal, Cité Descartes, Champs – sur – Marne, 77455 Marne – la – Vallée cedex 2, France

2: IRSTEA, Unité de Recherche RECOVER, 3275 route de Cézanne, CS 40061, 13182 Aix-en-Provence Cedex 5, France

Corresponding author:

Nadia BENAHMED

IRSTEA, Unité de Recherche RECOVER,

3275 route de Cézanne, CS 40061, 13182 Aix-en-Provence Cedex 5, France

Telephone: +33 4 42 66 99 04

Fax: +33 4 42 66 88 65

Email: nadia.benahmed@irstea.fr

Abstract

Bender elements technique has become a popular tool for determining shear wave velocity (V_s), hence the small-strain shear modulus of soils (G_{max}), thanks to its simplicity and non-destructive character among other advantages. Several methods were proposed to determine the first arrival of V_s. However, none of them can be widely adopted as a standard and there is still an uncertainty on the detection of the first arrival.

In this study, bender elements tests were performed on lime-treated soil and both shear wave and compression wave velocities at various frequencies were measured. In-depth analysis showed that the S-wave received signal presents an identical travel time and opposite polarity compared with that of the S-wave components in P-wave received signal, especially at high frequency. From this observation, a novel interpretation method based on the comparison between the S-wave and P-wave received signals at high frequency is proposed. This method enables the determination of the arrival time of S-wave objectively, avoiding less reliable arrival pick-up point. Furthermore, the "π-point" method and cross correlation method were also employed and the obtained results agree well with those from the proposed method, indicating the accuracy and reliability of the latter. The effects of frequency on the shear wave velocity are also discussed.

Keywords: bender elements; signal interpretation; shear wave; compression wave; S+P interpretation method

Introduction

The small-strain shear modulus (G_{max}) is a parameter of paramount importance in describing the elastic properties of soil. It is widely used in the analysis of dynamic problems in anti-seismic engineering (Zhou et al. 2005; Yang et al. 2009; Luke et al. 2013). It is also used to assess the soil stiffness in geo-environmental engineering (Tang et al. 2011; Gu et al. 2013; Hoyos et al. 2015). The value of G_{max} is usually determined from shear wave velocity (V_s) measurements either in the field or in the laboratory.

The measurement of V_s can be obtained from conventional laboratory experiments using resonant column (Hardin and Richart 1963; Anderson and Stokoe 1978; Fam et al. 2002), torsional shear tests (Iwasaki et al. 1978; Youn et al. 2008), flat transducers and accelerometers (Brignoli et al. 1996; Mulmi et al. 2008; Wicaksono et al. 2008) and piezoelectric bender elements technique (Dyvik and Madshus 1985; Viggiani and Atkinson 1995; Brignoli et al. 1996; Jovičić et al. 1996; Pennington et al. 2001; Lings and Greening 2001; Leong et al. 2005; Yamashita et al. 2009; Clayton 2011). The bender elements technique was first introduced by Shirley and Hampton (1978) and Shirley (1978) to soil testing, and due to its ability to measure the shear wave velocity of soil in a small-strain range, less than 0.001%, and in a wide range of stress conditions, it has taken a lot of interest of researchers. Nowadays, the bender elements transducers have been becoming a common laboratory tool, and have been incorporated in many geotechnical testing devices, such as oedometers (Dyvik and Olsen 1991; Zeng and Grolewski 2005; Sukolrat 2007), cubical and conventional triaxial apparatuses (Gajo et al. 1997; Jovičić and Coop 1998; Kuwano et al. 1999; Pennington et al. 2001; Fioravante and Capoferri 2001; Sukolrat et al. 2006; Leong et al. 2009; Finno and Cho 2011; Aris et al. 2012; Styler and Howie 2013), resonant column apparatuses (Ferreira et al. 2007; Youn et al. 2008; Gu et al. 2013).

Despite the popularity of its use, difficulties of signal interpretation of bender elements technique, mainly in the determination of the wave arrival time, are still remaining. Different methods and frameworks for the signal interpretation were reported (Lee and Santamarina 2005; Viana da Fonseca et al. 2009; Leong et al. 2009; Arroyo et al. 2010), but none has been widely accepted as a standard. In fact, the complex phenomena of wave propagation in a soil sample have not been clearly understood yet, which represents an obstacle to the determination of the arrival point accurately and objectively (Camacho-Tauta et al. 2013).

In the field of geotechnical engineering, most tested materials with bender elements are soils with low stiffness, and generally, the chosen frequency of excitation voltage in most studies ranges from 1 to 30 kHz (Lee and Santamarina 2005; Sukolrat 2007; Youn et al. 2008; Viana da Fonseca et al. 2009; Leong et al. 2009). A few researchers used the bender elements technique for stiffer materials, including sandstones (Alvarado 2007), cement treated clay (Hird and Chan 2008), and argillaceous rocks (Arroyo et al. 2010). In these cases, the working frequency range is different, and higher input frequency should be chosen due to the higher resonant frequency of stiff material (Lee and Santamarina 2005).

This technical note puts forward an objective method for the signal interpretation of bender elements technique, with respect to the determination of the first arrival time of shear wave. This method is based on the comparison of both S-wave and P-wave received signals obtained on the same sample with a single pair of bender elements to determine a unique arrival point. In this study, the bender elements tests were performed on compacted lime-treated silt samples extending, thus, this technique to stiff soils. The results obtained by the proposed method are validated by comparing with those of other methods.

Background

Working principal of Bender Elements

The bender elements are piezo-electrical transducers, which consist of two thin piezo-ceramic bimorph sheets with external conducting surfaces, mounted together with a conductive metal shim at the centre. Details of the connection are given in Figure 1a. When an input waveform voltage is applied on the S-wave transmitter, one piezoceramic sheet extends and the other contracts, leading the transmitter to bend and generate a shear wave signal. The S-wave receiver bends when the shear wave arrives, propagating an electrical signal that can be visualised and measured by a digital oscilloscope. The operation of bender elements for S-wave transmission was well described by other researchers (Dyvik and Madshus 1985; Lings and Greening 2001; Lee and Santamarina 2005; Camacho Tauta et al. 2012).

Lings and Greening (2001) introduced a bender-extender element to transmit and receive both S-wave and P-wave with a single pair of transducers. The bender (or S-wave) receiver and transmitter in bender element testing also act as an extender (or P-wave) transmitter and receiver, respectively. Specifically, when an input voltage is applied on the extender transmitter, both two piezoceramic sheets with opposite polarisations extend or contract at the same time, causing the propagation of P-wave in a longitudinal direction. The P-wave wiring and transmitting are illustrated in Figure 1b. Note that the measurement of P-wave velocity is mainly useful for unsaturated soils. Since in the saturated soils, P-wave usually travels much faster through water than through soil skeletion (Leong et al. 2009). Nevertheless, in this study, the degree of saturation of the tested material is lower than 95%. Bardet and Sayed (1993) who studied the Ottawa sand reported that the P-wave velocity became close to the value of dry sample when the degree of saturation decreased from 100% to 95%.

Determination of shear wave velocity

During bender elements testing, both the transmitted and received signals are recorded to determine the travel time, t, of S-wave through a sample. The shear wave velocity, V_s, can then be calculated from the tip-to-tip travel length between the bender elements, L_{tt}, and travel time, t, as follows (Viggiani and Atkinson, 1995):

$$V_s = \frac{L_{tt}}{t} \tag{1}$$

According to the theory of shear wave propagation in an elastic body, the small strain shear modulus, G_{max}, can be determined by the following formula:

$$G_{max} = \rho V_s^2 \tag{2}$$

where ρ is the density of soil sample.

Interpretation of bender element tests usually takes the advantage of the knowledge and experience gained into the development of in situ geophysical tests such as Down-Hole and Cross-Hole tests or even surface tests such as SASW tests (Stokoe et al. 2004; Viana da Fonseca et al. 2006).

Determination of travel time

An accurate determination of the travel time is a crucial issue to get a reliable value of V_s, hence G_{max}. The existing common methods for determining travel time can be classified into two categories: time domain and frequency domain methods.

The time domain methods determine the travel time directly from the time lag between the transmitted and received signals. Referring to different characteristic points, the time domain methods can be divided into “arrival-to-arrival” method, “peak-to-peak” method and “cross correlation method”.

The first method, based on the visual inspection of the received signal, is the most commonly used one; however, the determination of an accurate arrival point using this method is still controversial and quite subjective due to the complex received signal, wave’s reflexion and the near field effect. Many studies reported that the near field effect decreases with the increase of frequency or the ratio of the wave path length to wavelength, L_{tt}/λ. Arulnathan et al. (1998) reported that the near field effect disappears when this ratio is larger than 1. Pennington et al. (2001) pointed out that when the L_{tt}/λ values range from 2 to 10, a good signal can be obtained. Wang et al. (2007) advocated a ratio greater than or equal to 2 to avoid the near field effect. Similarly, a value of 3.33 was recommended by Leong et al. (2005) to improve the signal interpretation.

Figure 2 shows a typical single sinusoidal S-wave transmitted signal and its corresponding received signal. Generally, point “a” (the first deflection) is taken as the arrival of the near field component of received signal (Brignoli et al. 1996). Both point “b” (the first reversal) and point “c” (zero after first reversal) are chosen as the arrival points of S-wave by most researchers (Brignoli et al. 1996; Lee and Santamarina 2005; Youn et al. 2008; Yamashita et al. 2009; Arroyo et al. 2010).

The "peak-to-peak" method is also widely applied in the signal interpretation. In this method, time delay between the peak of transmitted signal and the first major peak of received signal (point "d" in Figure 2) is regarded as the travel time (Clayton et al. 2004; Ogino et al. 2015). Note that, since the frequency of received signal may be slightly different from that of transmitted signal, and that the nature of the soil and size of the sample often affect the shape of the signal which could present more than one peak, great attention should be paid to the calculation of travel time by the "peak-to-peak" method.

"Cross-correlation" method is another kind of time domain method. It assumes the travel time as the time shift corresponding to the peak value of cross-correlation function between the transmitted and received signals. The cross-correlation approach, first adopted by Viggiani and Atkinson (1995), is based on the following expression::

$$CC_{xy}(\tau) = \lim_{T \to \infty} \frac{1}{T} \int_0^T x^*(t) y(t+\tau) dt \tag{3}$$

where *x(t)* and *y(t)* are the received and transmitted signals respectively, *T* is the time record and τ is the time shift between two signals. First, the transmitted and received signals are converted to their linear spectrums using Fast Fourier Transform. Then the cross-power spectrum can be built based on the linear spectrum of received signal and the complex conjugate of the linear spectrum of transmitted signal. Eventually, the maximum of the cross-correlation function gives the travel time of shear wave. However, the accuracy of the cross-correlation method is largely dependent on the quality of received signals. Many limitations due to complex characteristics of received signal or incompatible transformation have been reported by several researchers (Arulnathan et al. 1998; Viana da Fonseca et al. 2009; Chan 2012).

Frequency domain methods estimate the travel time according to the relationship between the change in the phase angle, which corresponds to the phase shift between the transmitter and receiver signals, and input frequency (Greening and Nash 2004; Viana da Fonseca et al. 2009; Ogino et al. 2015). These methods can be applied using discrete method called "π-point" method (Greening and Nash 2004; Viana da Fonseca et al. 2009), or continuous method such as Frequency Spectral Analysis (Greening and Nash 2004; Viana da Fonseca et al. 2009; Kim et al. 2015). They were first performed on rock and mud samples by Kaarberg (1975) and later widely accepted by other researchers (Greening et al. 2003; Gutierrez 2007; Viana da Fonseca et al. 2009), thanks to their negligible effect of extraneous signals.

In the "π-point" method, a continuous sinusoidal wave at a single frequency is used as an input signal, the continuous sinuous wave transmitter and receiver are displayed in an X-Y plot on an oscilloscope, and the phase shift between these two signals is measured. The frequency of transmitter is increased very slightly from a low value, inducing a phase shift between the two signals. When these signals are in phase or out of phase, i.e. the phase differences are multiple N of π or (-π), the corresponding frequency, f, and the number of wavelength, N, are recorded.

It is well known that velocity, V, can be determined from the wavelength, λ, and the frequency (Viana da Fonseca et al. 2009):

$$V = \lambda f = f\frac{L}{N} \tag{4}$$

where the travel time, t, can be deduced from:

$$t = \frac{N}{f} \tag{5}$$

This indicates that the slope of the N-f plot represents the travel time.

Result given by this method is more objective than that obtained by time domain method. However, it has the drawbacks of time consuming and limited interpretable points (Viana da Fonseca et al. 2009).

Compared with the time-consuming "π-point" method, continuous method (Frequency Spectral Analysis) provides more available information in a short period of time with less effort. Continuous method applies a sweep signal which has a wide frequency spectrum (for example: 0 – 20 kHz) as input wave and uses a spectrum analyzer to establish the relationship between the frequency and the phase change, as introduced by Greening et al. (2003), Greening and Nash (2004) and explained in details by Kim et al. (2015). Specifically, the spectrum analyzer computes the coherence function between the transmitted and received signals. Based on the coherence function and phase angle it provides, the travel time can be determined directly from the slope of the linear line representing the relationship between the frequency and phase angle. However, further analysis is necessary when applying this method if the result convergence cannot be reached quickly (Viana da Fonseca et al. 2009).

Viana da Fonseca et al. (2009) also proposed a practical framework which combines both time-domain and frequency-domain methods for an enhanced interpretation of the bender element testing results. Nevertheless, the differences of the travel time determined by the time domain method and frequency domain method are quite large, and the causes are still not well understood (Greening et al. 2003; Greening and Nash 2004; Viana da Fonseca et al. 2009; Ogino et al. 2015). Therefore, there is still a strong need of searching a simple and objective approach for the bender element testing interpretation with a reliable determination of the arrival time.

In this study, the "arrival-to-arrival" method, "peak-to-peak" method, and "π-point" method are evaluated through the interpretation of signals obtained on compacted lime treated soils. Furthermore, based on the observation that the S-wave received signal presents an identical travel time and opposite polarity compared with that of the S-wave components in P-wave received signal, especially at high frequency, a novel method namely S+P method is proposed and its accuracy is proved by the comparison with "π-point" method.

Experimental methods

Tested Material

The soil used in this study was a plastic silt, taken from an experimental embankment with the ANR project TerDOUEST (Terrassements Durables - Ouvrages en Sols Traités, 2008 - 2012) at Héricourt, France. This soil was first air-dried, ground and sieved to 0.4 mm. Quicklime was used in the treatment. The soil powder was first mixed thoroughly with 2% lime, and then humidified to reach two target water contents (at dry or wet side of optimum). More details about the geotechnical properties of this silt and the preparation process of samples can be found in Wang et al. (2015). In this study, four compacted lime-treated samples (50 mm in diameter and 50 mm in height) with degree of saturation, S_r = 72 % at dry side and S_r = 93 % at wet side, were tested. The specific sample information is listed in Table 1.

Experimental Techniques

The bender element system used in this study consists of two bender elements (one S-wave transmitter/P-wave receiver and one S-wave receiver/P-wave transmitter, as shown in Figure 3), installed at the two extremities of the soil sample. Beforehand, a slot was carried out on the surface of each sample extremity with the same direction to facilitate the insertion of the protruded part of the bender elements, and a good alignment of the latter. Afterwards, the sample (50 mm in diameter and 50 mm in height) was placed on a home-made wooden sample holder (see Figure 4a) specially designed to forbid any wave transmission outside the soil sample, which may interfere with the signal arrival (Brignoli et al. 1996; Lee and Santamarina 2005). Additional force was provided by the holder to enhance a good contact between the benders and the sample. Special care was taken to avoid any cross-talk by improving the shielding and grounding of the system. The output signal (± 20V sine pulse) was generated by a function generator (*TTi* TG1010A) and amplified by a power amplifier. Both the transmitter and the receiver signals were captured with an oscilloscope (Agilent DSO-X 2004A). The set-up of the system used is presented in Figure 4a and details of the arrangement of devices are illustrated in Figure 4b. All the four different interpretation methods presented previously ("arrival-to-arrival", "peak-to-peak", "π-point" and S+P methods) were applied for each sample. As for the conventional "arrival-to-arrival" and "peak-to-peak" methods, a single pulse S-wave with various input frequency was used as transmitted signal. In S+P method, both S-wave and P-wave signals transmitted through the same sample by modifying the connection between the two benders, as illustrated in Figure 4b. A continuous sweep signal (frequency increased slowly from 20 kHz to 50 kHz) was applied in the "π-point" method.

Prior to testing, calibration of bender elements (tip-to-tip calibration) was carried out by holding the two benders (transmitter and receiver) in contact with each other directly without sample. Both S-wave transmitter and P-wave transmitter were generated to measure the delay times for these two transmitters (t_d_S = 5.5 μs and t_d_P = 3.5 μs). These delay times were accounted for in the calculation of travel time when applying the time domain method.

Experimental Results

Figure 5 presents the results of sample D1 with the time domain methods (conventional arrival-to-arrival method and peak-to-peak method). The S-wave transmitted signals with various frequencies are considered (dashed lines) and the S-wave received signals are presented in solid lines. In the arrival-to-arrival method, the first reversal in the received signal is chosen as the arrival point of S-wave. Besides, the first major peak is highlighted to calculate the time delay by the peak-to-peak method. It is observed that for the relatively low frequencies used here (f = 5, 10 and 15 kHz), the interpretation of these received signals is ambiguous because of the evident near field effect. However, the signals at higher frequencies, from 20 kHz to 50 kHz, become quite clear and the near field less marked. These cases correspond to a ratio of wave path length to wavelength, L_{tt}/λ, larger than or equal to 1.9, and are in good agreement with those reported in the literature (Sanchez-Salinero et al. 1986; Brignoli et al. 1996; Arulnathan et al. 1998; Pennington et al. 2001; Leong et al. 2005; Wang et al. 2007). The results obtained from the "π-point" method on the sample (w = 17%, with a curing time, t_c = 25 h) are shown in Figure 6. A good linear relationship between the number of wavelength and frequency is obtained. The travel time, t, can be determined as 0.1441 ms directly from the slope of the matched line, according to Equation 5. Additionally, the good linear relationship observed also highlights that the frequency ranging from 25 to 50 kHz is reasonable and suitable for the determination of shear wave velocity by the time domain method.

In Figure 7, the S-wave and P-wave transmitted signals and the corresponding received signals are gathered. The arrival point of S-wave received signal can be determined by referring to P-wave received signal. It is well known that P-wave component travels the fastest, thus arrives first before the S-wave received signal. Specifically, the arrival point of S-wave received signal (point S) corresponds to the initial main excursion (point S_p), which is in the opposite direction of movement compared to that of point S in the S-wave received signal. Apparently, the curvature of these points (S and S_p) becomes much sharper when the input frequency increases up to 40 or 50 kHz, as shown in Figure 7c and 7d. Furthermore, the arrival point of P-wave received signal (point P) just corresponds to the arrival point of the near field components (point P_s) in the S-wave received signal. This is in good agreement with the observation by Brignoli et al. 1996 - a "near field component" travelling at a similar velocity as P-wave was observed on a dry sample. Therefore, we propose this method, namely S+P method to determine the arrival point of S-wave: the arrival time is defined by point S (corresponding point S_p in the P-wave received signal).

To verify the accuracy of this S+P method, Figure 8 collects all data of shear wave velocity obtained from different interpretation methods. The results obtained from the S+P method are compared with those from other methods. Note that in the arrival-to-arrival method, point b (first reversal as mentioned above) is chosen as the arrival point of S-wave. As for the result by π-point method in Figure 8, the straight line represents a unique value of travel time which is determined as the input frequency slowly increasing from about 20 kHz to 50 kHz in each case. The differences between the shear wave velocities (V_s) obtained from the conventional time domain methods (arrival-to-arrival method and peak-to-peak method) and that from the "π-point" method are about 30%. Similar ranges of difference are reported by other researchers (Viggiani and Atkinson 1995; Viana da Fonseca et al. 2009; Ogino et al. 2015). Nevertheless, the difference between the results obtained from S+P method and that taken from "π-point" method is only around 10% in all tests; while this difference shows a good agreement between the results obtained from S+P method and those from cross correlation method, especially in the high frequency range, as illustrated in Figure 8. Therefore, the accuracy of the proposed method (S+P method) can be confirmed.

Discussions

The results obtained in this study show that the S-wave received signals are unreadable at lower frequencies (f = 5, 10 and 15 kHz), due to the influence of near field components. The effect of the latter is usually significant insofar as it obscures the shear wave arrival time point when the input frequency is low and the distance between the transmitter and receiver is short. Many researchers used the ratio of wave path length to wavelength L_{tt}/λ as an essential parameter to describe the near field effect. The near field effect can be reduced markedly with the increase of L_{tt}/λ, by improving the input frequency of transmitter or enlarging the distance between the transmitter and the receiver.

The results indicate also that the near field effect diminishes and a much clear received signal appears as the L_{tt}/λ value reaches 1.91 (in the arrival-to-arrival method). Similar conclusion can be made referring to the results of "π-point" method which shows a good linear relationship between the number of wavelength and frequency when the input frequency increases from 20 kHz (in case of L_{tt}/λ = 1.9).

A higher frequency makes the received signal more readable in case of testing on a stiff material such as compacted lime-treated silt. However, the P-wave component can become significant when the excitation frequency is high (Brignoli et al. 1996). This is different from a near field component (Lee and Santamarina 2005). Bender element can also generate small compressive displacements even though the main displacements produced are of shear nature (Brignoli et al. 1996). More importantly, the small compressive components (P-wave components) can be prominent in case of high frequency being excited on stiff materials, resulting in slight interference with the shear components (S-wave components) which have relatively slower travel velocity. Conversely, some shear displacements would be generated simultaneously with the major excitation of compressive displacements. Note that the polarity of S-wave components is always contrary to that of P-wave components in the same signal. It is even important that the travel velocity of S-wave components in P-wave received signal is identical with that of the S-wave received signals.

According to the analyses above, the determination of arrival point of S-wave received signals becomes clear and objective using the S+P method. That is, based on the comparison between S-wave and P-wave received signals, a unique point, S (as illustrated in Figure 7), can be identified and it corresponds to the arrival point of S-wave. This point located in

S-wave received signal, corresponding exactly to the point S_p in P-wave received signal, which shows opposite direction of movement in comparison with the point S in S-wave signal.

The results from S+P method show a small effect of input frequency (in a range from 20 to 50 kHz) on the shear wave velocity. As Figure 8 shows, shear wave velocity increases slightly as the input frequency increases. Similar phenomena were reported by other authors. Youn et al. (2008) pointed out that the shear wave velocity obtained from time domain method presents a small increasing trend with the increase of excitation frequency. Yamashita et al. (2009) also noted that the shear modulus increases with the increase of excitation frequency. To a certain extent, it might be a possible reason to explain why a slight decreasing trend of arrival time is observed when the excitation frequency increases. Specifically, when the frequency is relatively low (as shown in Figure 7a and 7b), point S determined by S+P method as the arrival point is not very clear. By contrast, in the case of high frequency (as shown in Figure 7c and 7d), point S is easy to be distinguished due to a sharp curvature at point S_p in the P-wave received signal. Brignoli et al. (1996) also recommended that high frequency should be used when measuring the P-wave components.

Conclusions

Due to the near field effect, reflected waves and soil properties, determining the shear wave arrival time accurately and reliably in bender elements testing is difficult and still controversial, and new methods need to be developed.

In this study, a novel method is proposed for a practical interpretation of the results from bender element tests, for unsaturated or nearly saturated soil specimen. This method, namely S+P method, is mainly based on the comparison between the S-wave and P-wave received signals, and enables the determination of the arrival point of S-wave signal in a more objective fashion. When a high frequency S-wave signal is excited, the P-wave components become evident, and are easy to be distinguished from the S-wave received signal. Note that the P-wave received signal also includes some S-wave components which arrive after the P-wave components. Based on the identical travel velocity of S-wave components in both S-wave received signal and P-wave received signal, and the opposite polarities between these two different S-wave components, a unique arrival point of S-wave can be determined. Comparisons between the results obtained by this method and those by the π-point method and cross correlation method were made, indicating the relevance of the proposed method. It is also worth noting that compared to the π-point method, the proposed method is less time consuming.

Acknowledgements

The authors wish to thank the China Scholarship Council (CSC) and Ecole des Ponts ParisTech for their financial supports. They also acknowledge the technical support provided by IRSTEA Aix-en-Provence.

References

Alvarado, G. 2007. Influence of Late Cementation on the Behaviour of Reservoir Sands. Diss. PhD thesis, Imperial College London.

Anderson, D. G. and Stokoe, K. H. 1978. Shear Modulus: A Time-Dependent Soil Property. In: Dynamic Geotechnical Testing, ASTM International.

Arroyo, M., Pineda, J. A. and Romero, E. 2010. Shear Wave Measurements Using Bender Elements in Argillaceous Rocks. Geotech. Test. J., Vol. 33, pp. 1-11.

Arulnathan, R., Boulanger, R. W. and Riemer, M. F. 1998. Analysis of Bender Element Tests. Geotech. Test. J., Vol. 21, No. 2, pp. 120-131.

Aris M., Benahmed N. and Bonelli S. 2012. A Laboratory Study on the Behaviour of Granular Material Using Bender Elements. Euro. J. Environ. Civil. Engineer., Vol. 16, No. 1, pp. 97-110.

Bardet, J. P. and Sayed, H. 1993. Velocity and Attenuation of Compressional Waves in Nearly Saturated Soils. Soil Dyn. Earthq. Eng., Vol. 12, No. 7, pp. 391-401.

Brignoli, E. G. M., Gotti, M. and Stokoe, K. H. 1996. Measurement of Shear Waves in Laboratory Specimens by Means of Piezoelectric Transducers. Geotech. Test. J., Vol. 19, pp. 384-397.

Camacho-Tauta, J. F., Reyes-Ortiz, O. J. and Jimenez Alvarez, J. D. 2013. Comparison between Resonant-Column and Bender Element Tests on Three Types of Soils. Dyna, Vol. 80, No. 182, pp. 163-172.

Camacho-Tauta, J. F., Jimenez Alvarez, J. D. and Reyes-Ortiz, O. J. 2012 A Procedure to Calibrate and Perform Bender Element Test. Dyna, Vol. 79, No. 176, pp. 10-18,.

Chan, C. M. 2012. Variations of Shear Wave Arrival Time in Unconfined Soil Specimens Measured with Bender Elements. Geotech. Geo. Eng., Vol. 30, No. 2, pp. 461-468.

Clayton, C. R. I., Theron, M. and Best, A. I. 2004. The Measurement of Vertical Shear-Wave Velocity Using Side-Mounted Bender Elements in the Triaxial Apparatus. Géotechnique, Vol. 54, No. 7, pp. 495-498.

Clayton, C. R. I. 2011. Stiffness at Small Strain: Research and Practice. Géotechnique, Vol. 61, No. 1, pp. 5-37.

Dyvik, R. and Madshus, C. 1985. Lab Measurements of G_{max} Using Bender Elements. Proceedings of the conference on the Advances in the Art of Testing Soil under Cyclic Conditions, New York: ASCE Geotechnical Engineering Division, pp. 186-196.

Dyvik, R. and Olsen, T. S.. 1991. G_{max} Measured in Oedometer and DSS tests Using Bender Elements. Publikasjon-Norges Geotekniske Institutt, Vol. 181, pp. 1-4.

Fam, M. A., Cascante, G., and Dusseault, M. B. 2002. Large and Small Strain Properties of Sands Subjected to Local Void Increase. J. Geotech. Geoenviron., *ASCE*, Vol. 128, No. 12, pp. 1018-1025.

Ferreira, C., Viana da Fonseca, A. and Santos. J. A. 2007. Comparison of Simultaneous Bender Element Test and Resonant Column Tests on Porto Residual Soils. Soil Stress-Strain Behavior: Measurement, Modeling and Anal*ysis*, Springer Netherlands, pp. 523-535.

Finno, R. and Cho, W. 2011. Recent Stress-History Effects on Compressible Chicago Glacial Clays. J. Geotech. Geoenviron. Eng., Vol. 137, No. 3, pp. 197-207.

Fioravante, V., and Capoferri, R. 2001. On the Use of Multi-Directional Piezoelectric Transducers in Triaxial Testing. J. Geotech. Test., Vol. 24, No. 3, pp. 243-255.

Gajo, A., Fedel, A. and Mongiovi, L. 1997. Experimental Analysis of the Effects of Fluid-Solid Coupling on the Velocity of Elastic Waves in Saturated Porous Media. Géotechnique, Vol. 47, No. 5, pp. 993-1008.

Greening, P. D., Nash, D. F. T., Benahmed, N., Viana da Fonseca A. and Ferreira, C. 2003. Comparison of Shear Wave Velocity Measurements in Different Materials Using Time and Frequency Domain Techniques. Proceedings of Deformation Characteristics of Geomaterials, Lyon, France, pp. 381-386.

Greening, P. D. and Nash, D. F. T. 2004. Frequency Domain Determinantion of G_0 Using Bender Elements. J. Geotech. Test., Vol. 27, No. 3, pp. 288-294.

Gu, X., Yang, J. and Huang, M. 2013. Laboratory Measurements of Small Strain Properties of Dry Sands by Bender Element. Soils Found., Vol. 53, No. 5, pp. 735-745.

Gutierrez, G. A. 2007. Influence of Late Cimentation on the Behaviour of Reservoir Sands. Diss. PhD thesis, Imperial College London.

Hardin, B. O. and Richart, Jr. F. E. 1963. Elastic Wave Velocities in Granular Soils. J. Soil Mech. Found. Div., Vol. 89, No. SM1, pp. 33-65.

Hird, C. and Chan, C. M. 2008. One-dimensional Compression Tests on Stabilized Clays

Incorporating Shear Wave Velocity Measurements. J. Geotech. Test., Vol. 31, No. 2, pp. 495.

Hoyos, L. R., Suescún-Florez, E. A. and Puppala, A. J. 2015. Stiffness of Intermediate Unsaturated Soil from Simultaneous Suction-Controlled Resonant Column and Bender Element Testing. Eng. Geol., Vol. 188, pp. 10-28.

Iwasaki, T., Tatsuoka, F. and Takagi, Y. 1978. Shear Moduli of Sands under Cyclic Torsional Shear Loading. Soils Found., Vol. 18, No. 1, pp. 39-56.

Jovičić, V., Coop, M. R. and Simić, M. 1996. Objective Criteria for Determining G_{max} from Bender Element Tests. Geotechnique, Vol. 46, No. 2, pp. 357-362.

Jovičić, V. and Coop, M. R. 1998. The Measurement of Stiffness Anisotropy in Clays with Bender Element Tests in the Triaxial Apparatus. J. Geotech. Test., Vol. 21, No. 1, pp. 3-10.

Kaarsberg, E. A. 1975. Elastic-wave Velocity Measurements in Rocks and Other Materials by Phase-delay Methods. Geophysics, Vol. 40, pp. 955-960.

Kim, T., Zapata-Medina, D. G. and Vega-Posada, C. A. 2015. Analysis of Bender Element Signals during Triaxial Testing. Revista Facultad de Ingeniería Universidad de Antioquia, No. 76, pp. 107-113.

Kuwano, R., Connolly T. M. and Jardine, R. J. 1999. Anisotropic Stiffness Measurements in a Stress-Path Triaxial Cell. J. Geotech. Test., Vol. 23, No. 2, pp. 141-57.

Lee, J. S. and Santamarina, J. C. 2005. Bender Elements: Performance and Signal Interpretation. J. Geotech. Geoenvironmental Eng., Vol. 131, pp. 1063-1070.

Leong, E. C., Yeo, S. H. and Rahardjo, H. 2005. Measuring Shear Wave Velocity Using Bender Element. Geotech. Test. J., Vol. 28, pp. 488-498.

Leong, E. C., Cahyadi, J. and Rahardjo, H. 2009. Measuring Shear and Compression Wave Velocities of Soil Using Bender–Extender Elements. Can. Geotech. J., Vol. 46, pp. 792-812.

Ling, M. L. and Greening, P. D. 2001. A Novel Bender/Extender Element for Soil Testing. Géotechnique, Vol. 51, No. 8, pp. 713-7.

Luke, B., Werkema, D., and Andersen, S. 2013. Laboratory Investigation of Seismic Effects of Nanoparticle Dispersions in Saturated Granular Media. Proceeding of the 18th International Conference on Soil Mechanics and Geotechnical Engineering, Paris.

Mulmi, S., Sato, T. and Kuwano, R. 2008. Performance of Plate Type Piezo-Ceramic Transducers for Elastic Wave Measurements in Laboratory Soil Specimens. Seisan Kenkyu, Vol. 60, No. 6, pp. 565-569.

Ogino, T., Kawaguchi, T., Yamashita, S. and Kawajiri, S. 2015. Measurement Deviations for Shear Wave Velocity of Bender Element Test Using Time Domain, Cross-Correlation, and Frequency Domain Approaches. Soils Found., Vol. 55, pp. 329-342.

Pennington, D. S., Nash, D. F. T. and Lings, M. L. 2001. Horizontally Mounted Bender Elements for Measuring Anistropic Shear Moduli in Triaxial Clay Specimens. Geotech. Test. J., Vol. 24, No. 2, pp. 133-144.

Sanchez-salinero, I., Roesset, J. M. and Stokoe, K. H. 1986 Analytical Studies of Body Wave Propagation and Attenuation. Geotechnical Engineering Report No. GR86-15, Texas Univ at Austin Geotechnical Engineering Center.

Shirley, D. J. 1978. An improved shear wave transducer. J. Acoust. Soc. Am., Vol. 63, No. 5, pp. 1643-1645.

Shirley, D. J. and Hampton, L. D. 1978. Shear Wave Measurements in Laboratory Sediments. J. Acoust. Soc. Am., Vol. 63, No. 2, pp. 607-613.

Stokoe, K. H. Joh, S. H. and Woods, R. D. 2004. Some Contributions of in situ Geophysical Measurements to Solving Geotechnical Engineering Problems. Proceedings of ISC-2: Geotechnical and Geophysical Site Characterization. Viana da Fonseca and Mayne, Eds., Porto, Portugal, 19-22 September, Millpress Science Publishers, Rotterdam, Netherlands. Vol. 1, pp. 97-132.

Styler M. A. and Howie, J. A. 2013 Continuous Monitoring of Bender Element Shear Wave Velocities During Triaxial Testing. Geotech. Test. J., Vol. 36, No. 5, pp. 649-659.

Sukolrat J., Nash D.F.T., Ling, M.L. and Benahmed N. 2006 The Assessment of Destructuration of Bothkennar Clay Using Bender Elements. In Soft Soil Engineering: Proceedings of the Fourth International Conference on Soft Soil Engineering, Vancouver, Canada, pp.471.

Sukolrat J. 2007. Structure and Destructuration of Bothkennar Clay. Diss. PhD thesis, University of Bristol.

Tang, A., Vu, M. and Cui, Y. 2011. Effects of the Maximum Grain Size and Cyclic Wetting/Drying on the Stiffness of a Lime-Treated Clayey Soil. Géotechnique, Vol. 61, No. 5, pp. 421-429.

Viana da Fonseca, A. V., Carvalho, J., Ferreira, C., Santos, J. A., Almeida, F., Pereira, E., Feliciano, J., Grade, J. and Oliveira, A. 2006. Characterization of a Profile of Residual Soil from Granite Combining Geological, Geophysical and Mechanical Testing Techniques. Geotech. Geologic. Eng., Vol. 24, No. 5, pp.1307–1348.

Viana da Fonseca, A. V., Ferreira, C. and Fahey, M. 2009. A Framework Interpreting Bender Element Tests, Combining Time-Domain and Frequency-Domain Methods. Geotech.

Test. J., Vol. 32, pp. 91-107.

Viggiani, G. and Atkinson, J. H. 1995. Interpretation of Bender Element Tests. Géotechnique, Vol. 45, No. 1, pp. 149-154.

Wang, Y., Cui, Y. J., Tang, A. M., Tang, C. S. and Benahmed, N. 2015. Effects of Aggregate Size on Water Retention Capacity and Microstructure of Lime-Treated Silty Soil. Geotech. Lett., Vol. 5, No. 4, pp. 269-274.

Wang, Y. H., Lo K. F., Yan, W. M. and Dong, X. B. 2007. Measurement Biases in the Bender Element Test. J. Geotech. Geoenviron. Eng., Vol. 133, No. 5, pp. 564-574.

Wicaksono, R. I., Tsutsumi, Y., Sato, T., Koseki, J. and Kuwano, R.. 2008. Stiffness Measurements by Cyclic Loading, Triggger Accelerometer, and Bender Element on Sand & Gravel. Deformational Characteristics of Geomaterials, Atlanta, GA, Vol. 2, pp. 733-39.

Yamashita, S., Kawaguchi, T., Nakata, Y., Mikami, T., Fujiwara, T. and Shibuya, S. 2009. Interpretation of International Parallel Test on the Measurement of G_{max} Using Bender Elements. Soils Found., Vol. 49, pp. 631-650.

Yang, J. and Yan, X. R. 2009. Site Response to Multi-Directional Earthquake Loading: A Practical Procedure. Soil. Dyn. Earthq. Eng., Vol. 29, No. 4, pp. 710-721.

Youn, J. U., Choo, Y. W. and Kim, D. S. 2008. Measurement of Small-Strain Shear Modulus G_{max} of Dry and Saturated Sands by Bender Element, Resonant Column, and Torsional Shear Tests. Can. Geotech. J., Vol. 45, pp. 1426-1438.

Zeng, X. W., and Grolewski, B. 2005. Measurement of G_{max} and Estimation of K_0 of Saturated Clay Using Bender Elements in an Oedometer. Geotech. Test. J., Vol. 28, No. 3, pp. 264-274.

Zhou, Y. G., Chen, Y. M and Huang, B. 2005. Experimental Study of Seismic Cyclic Loading Effects on Small Strain Shear Modulus of Saturated Sands. J. Zhejiang Univ. Sci. A., Vol. 6, No. 3, pp. 229-236.

List of Tables

List of Figures

Table 1 Sample characteristics

Sample	Dry density (Mg/m^3)	Water content (%)	Degree of saturation (%)	Curing time (Hours)
D1	1.65	17	72	25
D2	1.65	17	72	528
W1	1.65	22	93	27
W2	1.65	22	93	504

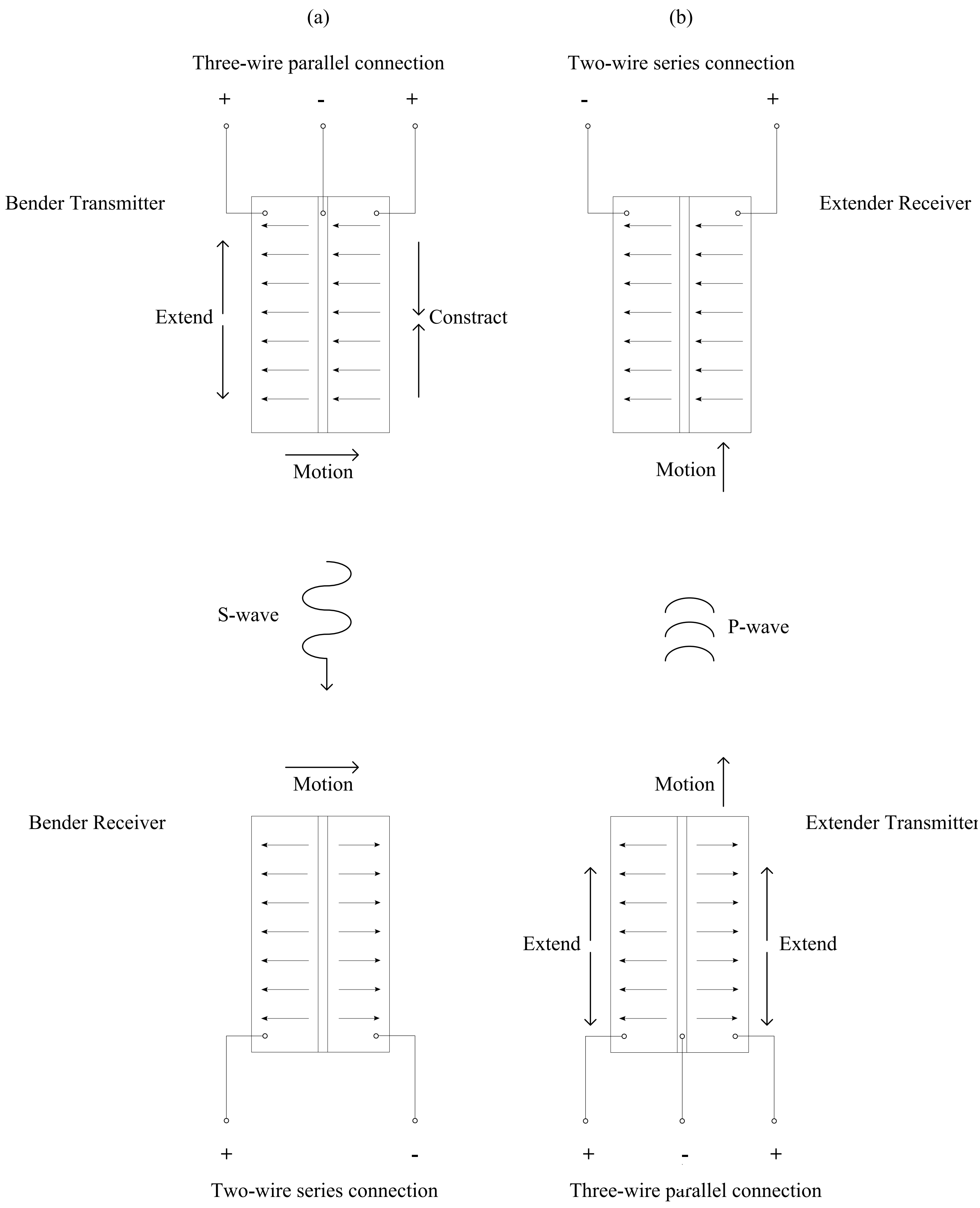

Figure 1. Sketch of bender and extender connection: (a) transmitting S-wave; (b) transmitting P-wave (after Lings and Greening 2001)

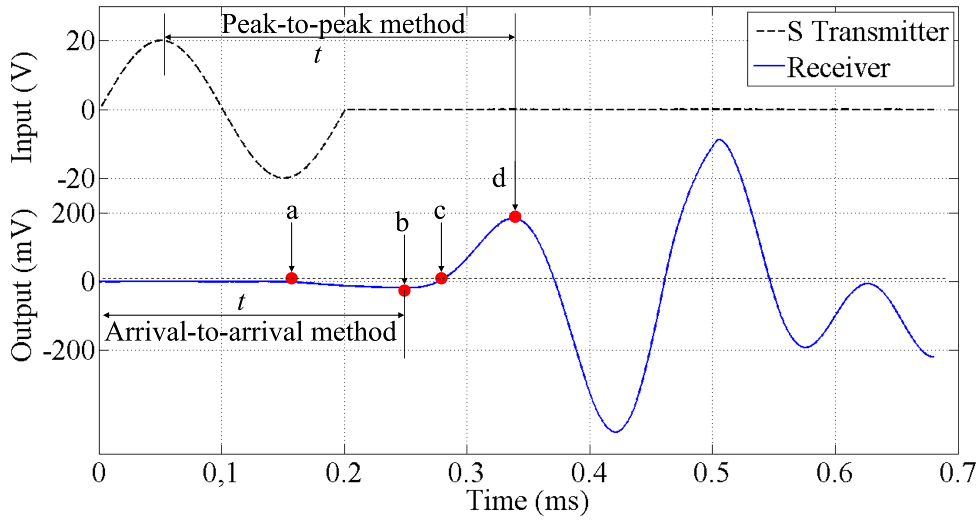

Figure 2. Typical S-wave transmitted and received signals

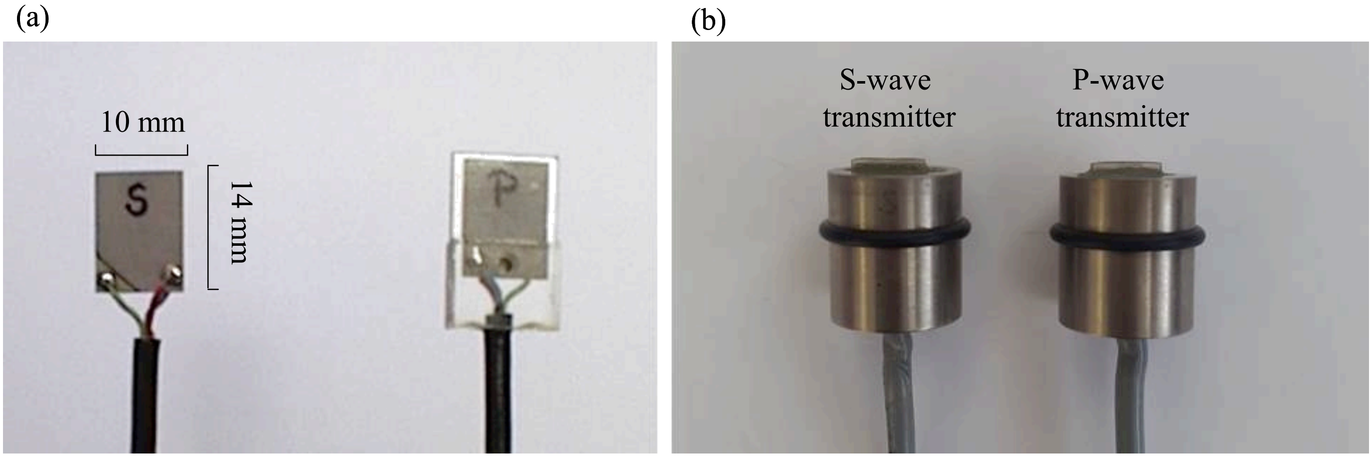

Figure 3. Bender elements transducers: (a) wiring of two bender elements; (b) GDS bender elements waterproofed and encapsulated in pot

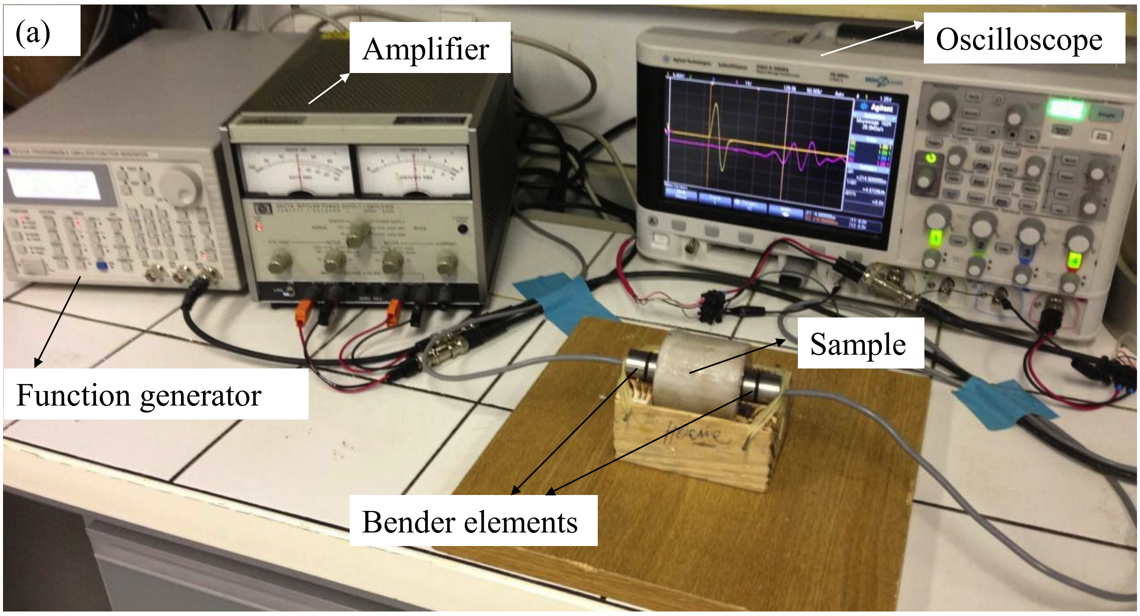

Figure 4. Setup of the bender element testing: (a) photo of the setup; (b) schematic diagram of the setup

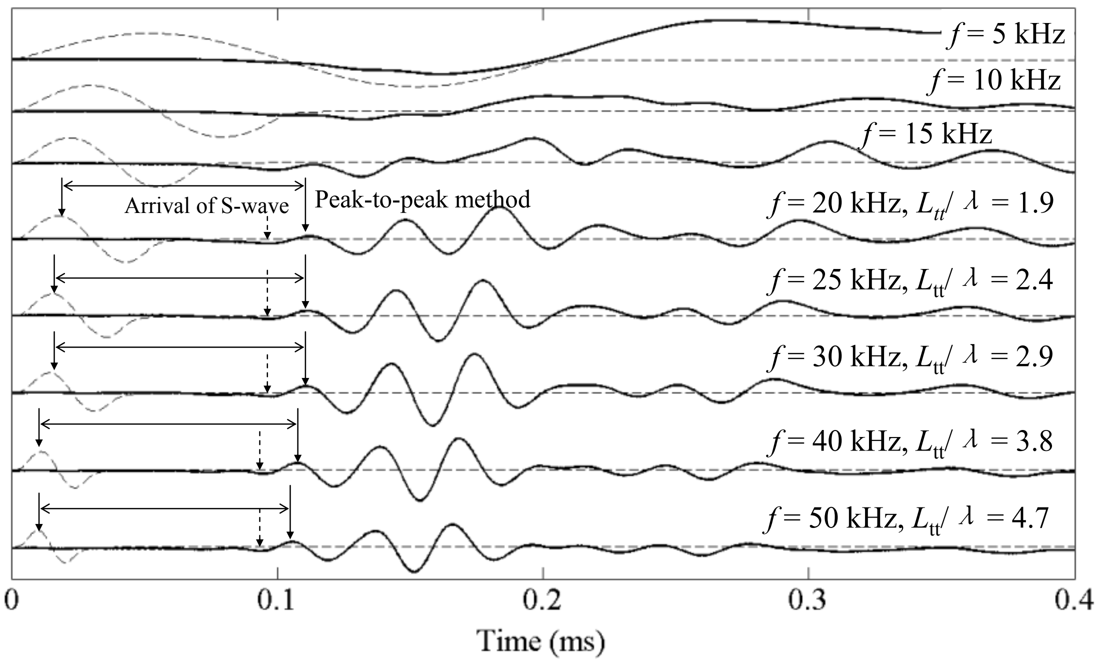

Figure 5. Measurements by traditional time domain methods (arrival-to-arrival method and peak-to-peak method) at different frequencies on a lime-treated sample (D1)

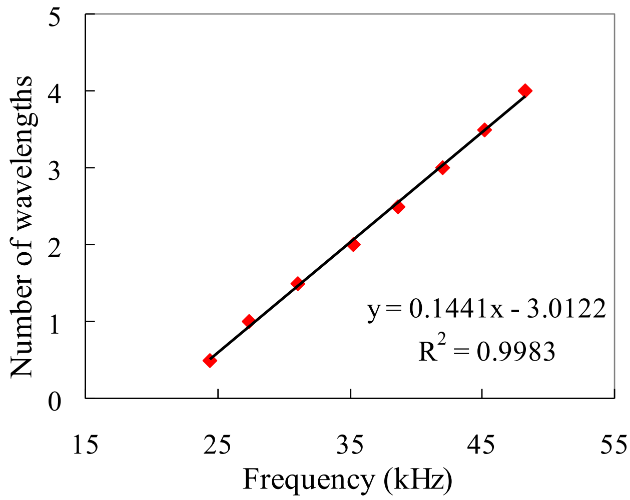

Figure 6. Measurements by “π-point” method on a lime-treated soil (D1)

(a)

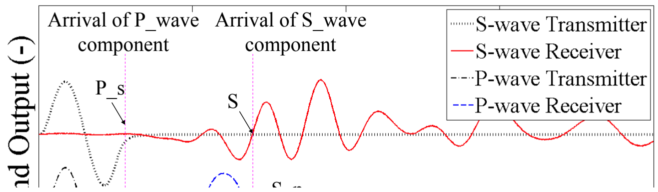
Arrival of P_wave component
Arrival of S_wave component
S-wave Transmitter
S-wave Receiver
P-wave Transmitter
P-wave Receiver
P_s
S
nd Output (-)

(b)

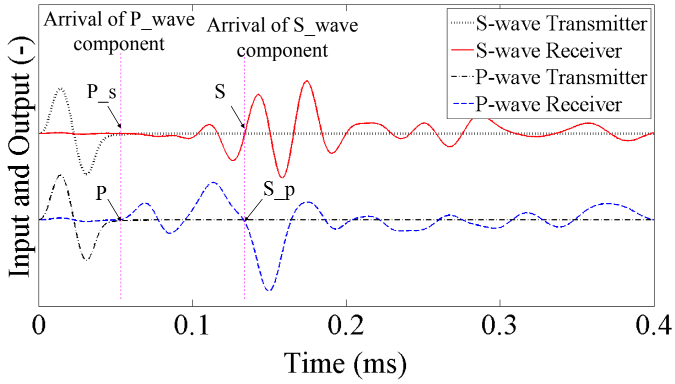
Arrival of P_wave component
Arrival of S_wave component
S-wave Transmitter
S-wave Receiver
P-wave Transmitter
P-wave Receiver
P_s
S
P
S_p
Input and Output (-)
0
0.1
0.2
0.3
0.4
Time (ms)

(c)

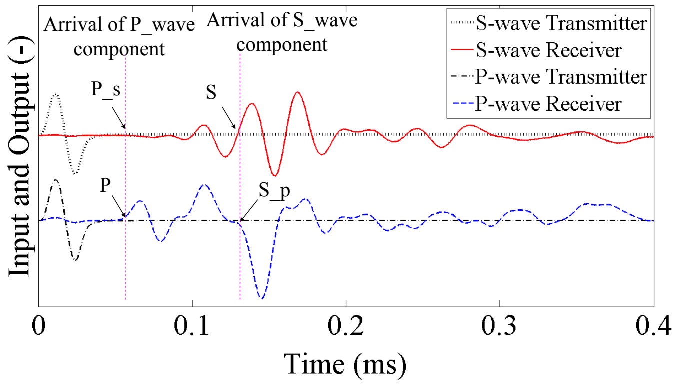
Arrival of P_wave component
Arrival of S_wave component
S-wave Transmitter
S-wave Receiver
P-wave Transmitter
P-wave Receiver
P_s
S
P
S_p
Input and Output (-)
0
0.1
0.2
0.3
0.4
Time (ms)

(d)

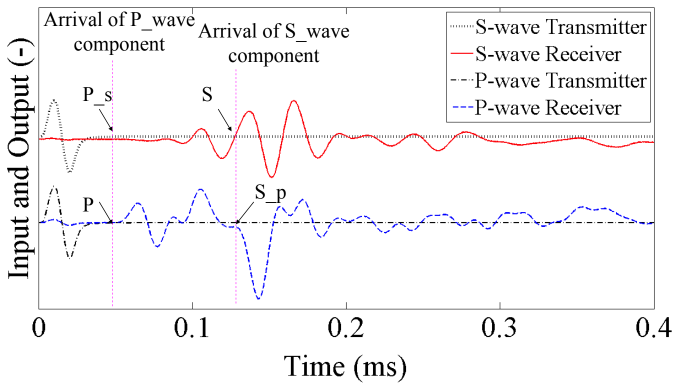
Arrival of P_wave component
Arrival of S_wave component
S-wave Transmitter
S-wave Receiver
P-wave Transmitter
P-wave Receiver
P_s
S
P
S_p
Input and Output (-)
0
0.1
0.2
0.3
0.4
Time (ms)

Figure 7. Determination of the arrival point by S+P method on a lime-treated soil (D1): (a) *f* = 20 kHz; (b) *f* = 30 kHz; (c) *f* = 40 kHz; (d) *f* = 50 kHz

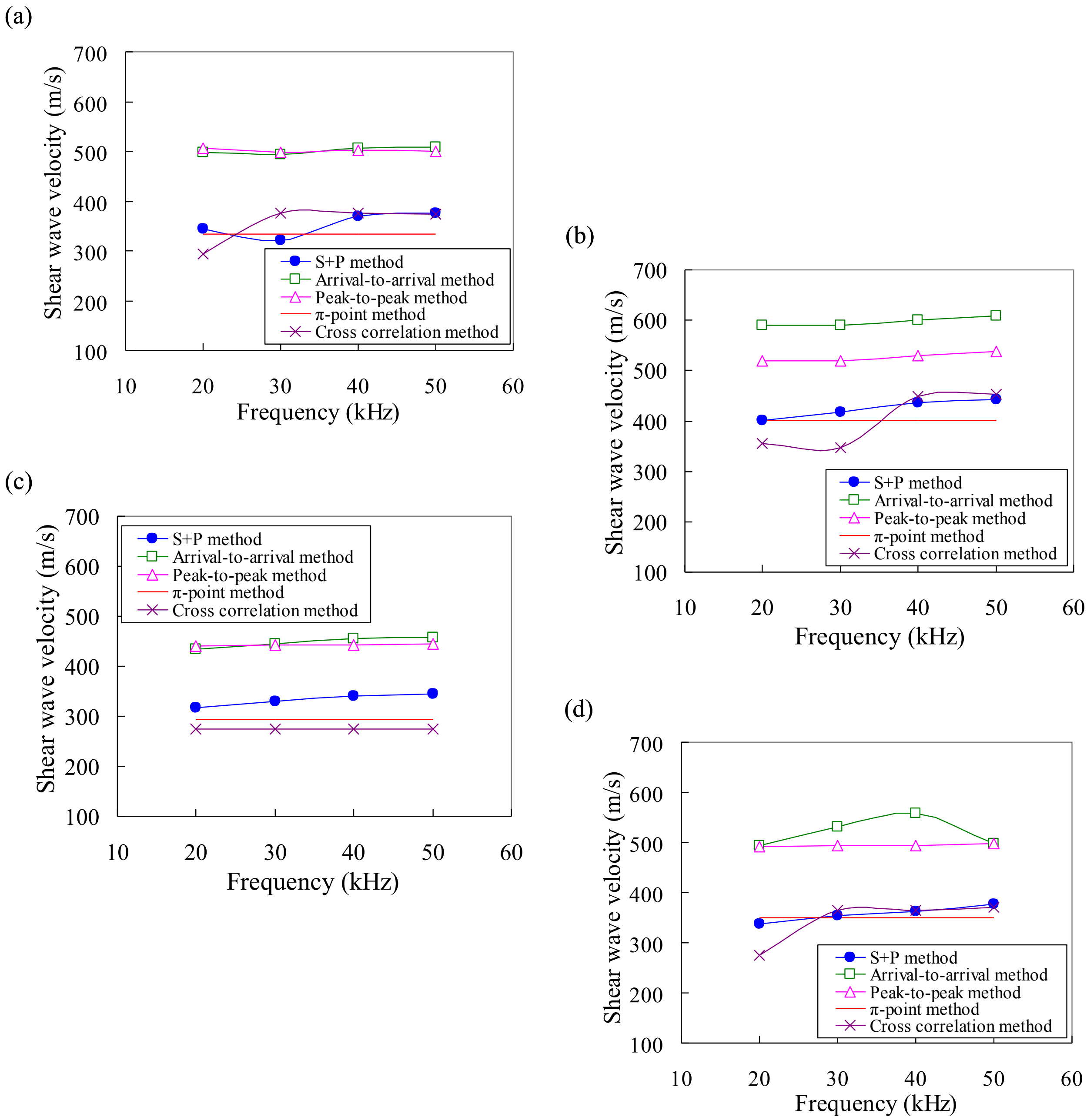

Figure 8. Comparisons of the measurements of shear wave velocity by different methods: (a) D1; (b) D2; (c) W1; (d) W2